Hindawi Publishing Corporation
Journal of Biomedicine and Biotechnology
Volume 2012, Article ID 735368, 11 pages
doi:10.1155/2012/735368

Research Article

Characterization of Flavonol Inhibition of DnaB Helicase: Real-Time Monitoring, Structural Modeling, and Proposed Mechanism

Hsin-Hsien Lin[1] and Cheng-Yang Huang[1,2]

[1] *Department of Biomedical Sciences, Chung Shan Medical University, No. 110, Section 1, Chien-Kuo N. Road, Taichung City 40201, Taiwan*
[2] *Department of Medical Research, Chung Shan Medical University Hospital, No. 110, Section 1, Chien-Kuo N. Road, Taichung City 40201, Taiwan*

Correspondence should be addressed to Cheng-Yang Huang, cyhuang@csmu.edu.tw

Received 1 February 2012; Revised 18 April 2012; Accepted 22 May 2012

Academic Editor: S. L. Mowbray

DnaB helicases are motor proteins essential for DNA replication, repair, and recombination and may be a promising target for developing new drugs for antibiotic-resistant bacteria. Previously, we established that flavonols significantly decreased the binding ability of *Klebsiella pneumoniae* DnaB helicase (*Kp*DnaB) to dNTP. Here, we further investigated the effect of flavonols on the inhibition of the ssDNA binding, ATPase activity, and dsDNA-unwinding activity of *Kp*DnaB. The ssDNA-stimulated ATPase activity of *Kp*DnaB was decreased to 59%, 75%, 65%, and 57%, in the presence of myricetin, quercetin, kaempferol, and galangin, respectively. The ssDNA-binding activity of *Kp*DnaB was only slightly decreased by flavonols. We used a continuous fluorescence assay, based on fluorescence resonance energy transfer (FRET), for real-time monitoring of *Kp*DnaB helicase activity in the absence and presence of flavonols. Using this assay, the flavonol-mediated inhibition of the dsDNA-unwinding activity of *Kp*DnaB was observed. Modeled structures of bound and unbound DNA showed flavonols binding to *Kp*DnaB with distinct poses. In addition, these structural models indicated that L214 is a key residue in binding any flavonol. On the basis of these results, we proposed mechanisms for flavonol inhibition of DNA helicase. The resulting information may be useful in designing compounds that target *K. pneumoniae* and other bacterial DnaB helicases.

1. Introduction

DNA helicases are motor proteins that play essential roles in DNA replication, repair, and recombination [1, 2]. In the replicative hexameric helicase, the fundamental reaction is the unwinding of double-stranded DNA (dsDNA) into single-stranded DNA (ssDNA) intermediates to provide ssDNA templates for DNA polymerases at the replication fork [3]. The most widely studied replicative helicase is *Escherichia coli* DnaB helicase (*Ec*DnaB) [4]. *Ec*DnaB participates in the initiation of DNA replication once the *oriC* region of *E. coli* is bound by the DnaA initiator protein [5, 6]. It continues to act during the priming and elongation phases of DNA replication, and it catalyzes ATP hydrolysis and migrates on the DNA template with a strict 5′-3′ direction [5]. ATP hydrolysis may drive the movement of the helicase toward the 3′ end of the lagging strand [7].

Currently, infections occur that are resistant to all antibacterial options [8]. Few therapies are effective against the six antibiotic-resistant ESKAPE pathogens (*Enterococcus faecium*, *Staphylococcus aureus*, *Klebsiella pneumoniae*, *Acinetobacter baumannii*, *Pseudomonas aeruginosa*, and *Enterobacter* species) [9, 10]. *K. pneumoniae* (*Kp*) is a ubiquitous opportunistic pathogen that causes severe diseases such as septicemia, pneumonia, urinary tract infections, and soft tissue infections [11]. Since DnaB helicase is required for DNA replication, blocking the activity of DnaB helicase would be detrimental to bacterial survival [12]. In addition,

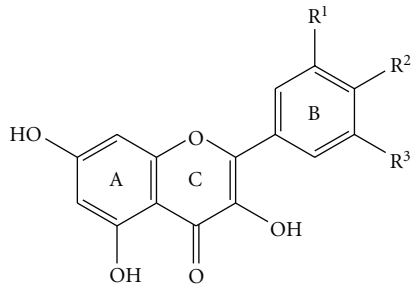

	R^1	R^2	R^3
Galangin	H	H	H
Kaempferol	H	OH	H
Quercetin	OH	OH	H
Myricetin	OH	OH	OH

Figure 1: Molecular structure of myricetin (Myr), quercetin (Que), kaempferol (Kae), and galangin (Gal).

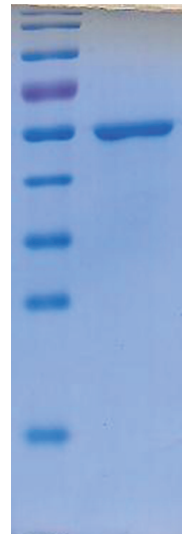

Figure 2: Coomassie Blue-stained SDS-PAGE (12%) of the purified *Kp*DnaB and molecular mass standards. The sizes of the standard proteins, from the top down, are as follows: 170, 130, 100, 70, 55, 40, 35, 25, and 15 kDa.

because the structure and function between eukaryotic and prokaryotic DnaB-like helicases are different [5, 12], the *K. pneumoniae* DnaB helicase (*Kp*DnaB) and other bacterial DnaB-like proteins may be a promising target in developing antibiotics.

Previously, we determined the three-dimensional structures of the *Geobacillus kaustophilus* DnaB-family protein (*Gk*DnaB) and its complex with ssDNA [7]. Although the overall structure of the apo and the complex forms of *Gk*DnaB is similar, the largest difference is found in their loop I region, which undergoes a strong conformational change during the helicase's action [7]. These structural and functional analyses are useful in helping our understanding of the mechanism of DNA translocation in replication forks, and the resulting information may be useful in designing compounds that target bacterial DnaB helicases. Recently, we established that the 4 flavonols (Figure 1) myricetin (Myr), quercetin (Que), kaempferol (Kae), and galangin (Gal) can interact with *Kp*DnaB and prevent dNTP binding [13]. Flavonoids are the most common group of plant polyphenols, and are responsible for much of the flavor and color of fruits and vegetables [14]. Over 5000 different flavonoids have been described; many of these compounds display structure-dependent biological and pharmacological activities [15]. The 6 major subclasses of flavonoids are flavonols, flavones, flavanones, flavanols, anthocyanidins, and isoflavones [14]. Flavonols, composed of 2 aromatic rings linked by a heterocyclic pyran-4-one ring, are known to have antioxidant [16], antiradical [17], and antibacterial activities [18]. In the present study, we further investigated the effect of flavonols on the inhibition of the ssDNA binding, ATPase activity, and dsDNA-unwinding activity of *Kp*DnaB. A new assay that enables the real-time measurement of DNA helicase activity was also developed. This assay may be useful for screening helicase inhibitors at high throughput.

2. Materials and Method

2.1. Materials. All restriction enzymes and DNA-modifying enzymes were purchased from New England Biolabs (Ipswich, MA, USA) unless explicitly stated otherwise. All custom oligonucleotide primers were obtained from Invitrogen Corporation (Carlsbad, CA, USA). All chemicals were purchased from Sigma-Aldrich (St. Louis, MO, USA) unless explicitly stated otherwise.

2.2. Protein Expression and Purification. The encoding region of *Kp*DnaB was put on pET21e expression vector and expressed with a hexahistidine tag at the C-terminus of the recombinant protein. The pET21e vector [19] was engineered from the pET21b vector (Novagen Inc., Madison, WI, USA), to avoid having the N-terminal T7 tag fused with the gene product. Details of the construction of pET21e-*Kp*DnaB expression vector and protein purification have been described previously [13]. The purified protein was dialyzed against Buffer B (20 mM HEPES, 100 mM NaCl; pH 7.0), and concentrated to 5 mg/mL. Protein purity remained greater than 95% as determined by Coomassie-stained SDS-PAGE (Figure 2).

2.3. Gel Shifts. EMSA for *Kp*DnaB was carried out using the same protocol as described previously for SSB proteins [20–22], with a minor modification. ssDNA oligonucleotides were custom synthesized by MdBio, Inc., Frederick, MD, USA. Radiolabeling was carried out with [γ^{32}P]ATP (6000 Ci/mmol; PerkinElmer Life Sciences) and T4 polynucleotide kinase (Promega, Madison, WI, USA). *Kp*DnaB (0, 90, 170, 340, 680, 1360, 2730, and 5450 nM) was incubated for 30 min at 25°C with 1.7 nM ssDNA substrate (dT30) and 16.7 μM flavonol in a total volume of 10 μL in 20 mM HEPES (pH 7.0) and 100 mM NaCl. Aliquots (5 μL) were

removed from each reaction solution and added to 2 μL of gel-loading solution (0.25% bromophenol blue and 40% sucrose, w/v). The resulting samples were resolved on a native 8% polyacrylamide gel (8.3 × 7.3 cm) at 4°C in TBE buffer (89 mM Tris borate and 1 mM EDTA) for 1 h at 100 V and visualized by phosphorimaging. The phosphor storage plate was scanned, and the data for complexed and free DNA bands were digitized for quantitative analysis. The ssDNA binding ability ($K_{d,app}$ value) for the protein was estimated from the protein concentration that binds 50% of the input DNA [23–25]. Each K_d value is calculated as the average of at least three measurements ± S.D.

2.4. FRET-Based dsDNA Unwinding Activity Assay. To monitor the 5′-3′ DNA helicase activity of *Kp*DnaB in real-time, we developed an assay on the basis of fluorescence resonance energy transfer (FRET) method. The dsDNA substrate was prepared with the fluorescent strand, 5′-TAGTACCGCCACCCTCAGAACC-3′ with Alexa Fluor 488 (maximum excitation/emission = 495/519 nm) coupled to the 5′-end, and the complementary quencher strand, 3′-ATCATGGCGGTGGGAGTCTTGGTTTTTTTTTTTTTT-5′ with BHQ1 coupled to the 3′-end, at a 1 : 1.2 concentration ratio. The dsDNA substrate was formed in 20 mM HEPES (pH 7.0) and 100 mM NaCl, by brief heating at 95°C for 5 min and then followed by slow cooling to room temperature overnight. The fluorescence helicase assay was performed in 20 mM HEPES (pH 7.0), 100 mM NaCl, 3 mM $MgCl_2$, 50 nM dsDNA substrate, and 5 mM ATP in 2.0 mL of reaction volume. The unwinding reaction was started by adding *Kp*DnaB (200 nM) and was carried out at 37°C for 60 min using a spectrofluorimeter (Hitachi F-2700; Hitachi High-Technologies, Tokyo, Japan). The fluorescence intensity was recorded every 5 s. The DNA helicase activity was calculated as the initial reaction velocity from the linear part of the progress curve using the linear regression method.

2.5. ATPase Activity Assay. The protocol for measuring the ATPase activity of purified *Kp*DnaB is based on the colorimetric determination of inorganic phosphate (Pi) released by the hydrolysis of ATP [26]. The ATPase activity assay for *Kp*DnaB (20–50 ng) was performed in 20 mM HEPES (pH 7.0), 100 pmol of ϕX-ssDNA, 10 μM flavonol, 100 mM NaCl, 3 mM $MgCl_2$, and 5 mM ATP in 100 μL of reaction volume. Liberated Pi was detected using ammonium molybdate and malachite green solutions, and absorbance was measured at 610 nm using a UV/vis spectrophotometer (Thermo Scientific Helios Omega; Thermo Fisher Scientific Inc., Waltham, MA, USA). The ATPase activity of *Kp*DnaB was calibrated with sodium phosphate (NaH_2PO_4) of known concentrations.

2.6. Bioinformatics. The amino acid sequences of *Kp*DnaB, *Ec*DnaB, *Gs*DnaB, and *Gk*DnaB were aligned using CLUSTALW2 [27]. The model of *Kp*DnaB was built from the coordinates of 2R6D (crystal structure of *Gs*DnaB), 2VYF (crystal structure of *Gk*DnaB), and 2VYE (crystal structure of *Gk*DnaB in complex with ssDNA) by using SWISS-MODEL, http://swissmodel.expasy.org/ [28]. The coordinate and topology file of the flavonols, Myr, Que, Kae, and Gal, was found in DrugBank, http://www.drugbank.ca/ [29]. The flavonol was individually computationally docked into the three-dimensional models of *Kp*DnaB by using PatchDock, http://bioinfo3d.cs.tau.ac.il/PatchDock/ [30]. The structures were visualized by using the program PyMol.

3. Results

3.1. Sequence Analysis. The gene *KPN04439*, encoding *K. pneumoniae* DnaB helicase, was initially found using a database search through the National Center for Biotechnology Information (NCBI). Based on the known nucleotide sequence, the predicted *Kp*DnaB monomer protein has a length of 471 amino acid residues and a molecular mass of 52.5 kDa, with a pI of 4.93. Analysis of the primary structure of *Kp*DnaB revealed the presence of the putative Walker A motif (aa 232–238), Walker B motif (aa 340–343), ATP binding sites (aa 237–238, 343, 384, 420, 442, and 453), and DNA binding sites (348, 349, 356–358, 383–391, 419-420, and 432-433); these are common in all known DnaB helicases. Figure 3 shows an alignment of the amino acid sequences of *K. pneumoniae* [13], *E. coli* [31], *Geobacillus stearothermophilus* [32], and *Geobacillus kaustophilus* DnaB helicases [7]; their ATP (boxed) and DNA binding sites (shaded in gray) are highly conserved.

3.2. ssDNA-Dependent ATPase Activity of KpDnaB. The ATPase activity of purified *Kp*DnaB is based on the vanadate-sensitive colorimetric determination of inorganic phosphate released by the hydrolysis of ATP [26]. Figure 4(a) shows a standard linear regression curve generated by plotting the optical density (OD) at 610 nm against the concentrations of sodium phosphate (NaH_2PO_4). After some preliminary experiments to establish a suitable range of concentrations for the reagents (including *Kp*DnaB) used for the assay, 3 mM $MgCl_2$, 5 mM ATP, 10 μM flavonol, and 20–50 ng of *Kp*DnaB were chosen for analysis of inhibition of *Kp*DnaB ATPase activity by the flavonol. In the absence of the flavonol and ϕX-ssDNA, the specific activity of *Kp*DnaB was $0.42 \pm 0.09\,\mu\text{mol}\cdot\text{min}^{-1}\cdot\text{mg}^{-1}$. In the presence of ϕX-ssDNA, the specific activity of *Kp*DnaB was increased to $5.5 \pm 0.6\,\mu\text{mol}\cdot\text{min}^{-1}\cdot\text{mg}^{-1}$. These data are similar to reported values for *Ec*DnaB; the activity of *Ec*DnaB is 3.3×10^5 (without M13 ssDNA) and 6.4×10^6 $\text{pmol}\cdot\text{min}^{-1}\cdot\text{mg}^{-1}$ (with M13 ssDNA), respectively, [33]. Thus, the ATPase activity of *Kp*DnaB was stimulated by ssDNA, a property common to all DnaB helicases.

3.3. ATPase Activity of KpDnaB Is Inhibited by Flavonols. Previously, we showed that the binding of *Kp*DnaB to dNTP is inhibited by the flavonols Myr, Kae, Gal, and Que [13]. Here, as shown in Figure 4(b), the ATP hydrolysis activity of *Kp*DnaB was also inhibited by the flavonols. In the presence of Myr, Que, Kae, or Gal, the specific activity of *Kp*DnaB was decreased to 59%, 75%, 65%, and 57%, respectively, meaning that Gal exhibited the strongest inhibitory effect on the ATP hydrolysis of *Kp*DnaB in the presence of ϕX-ssDNA.

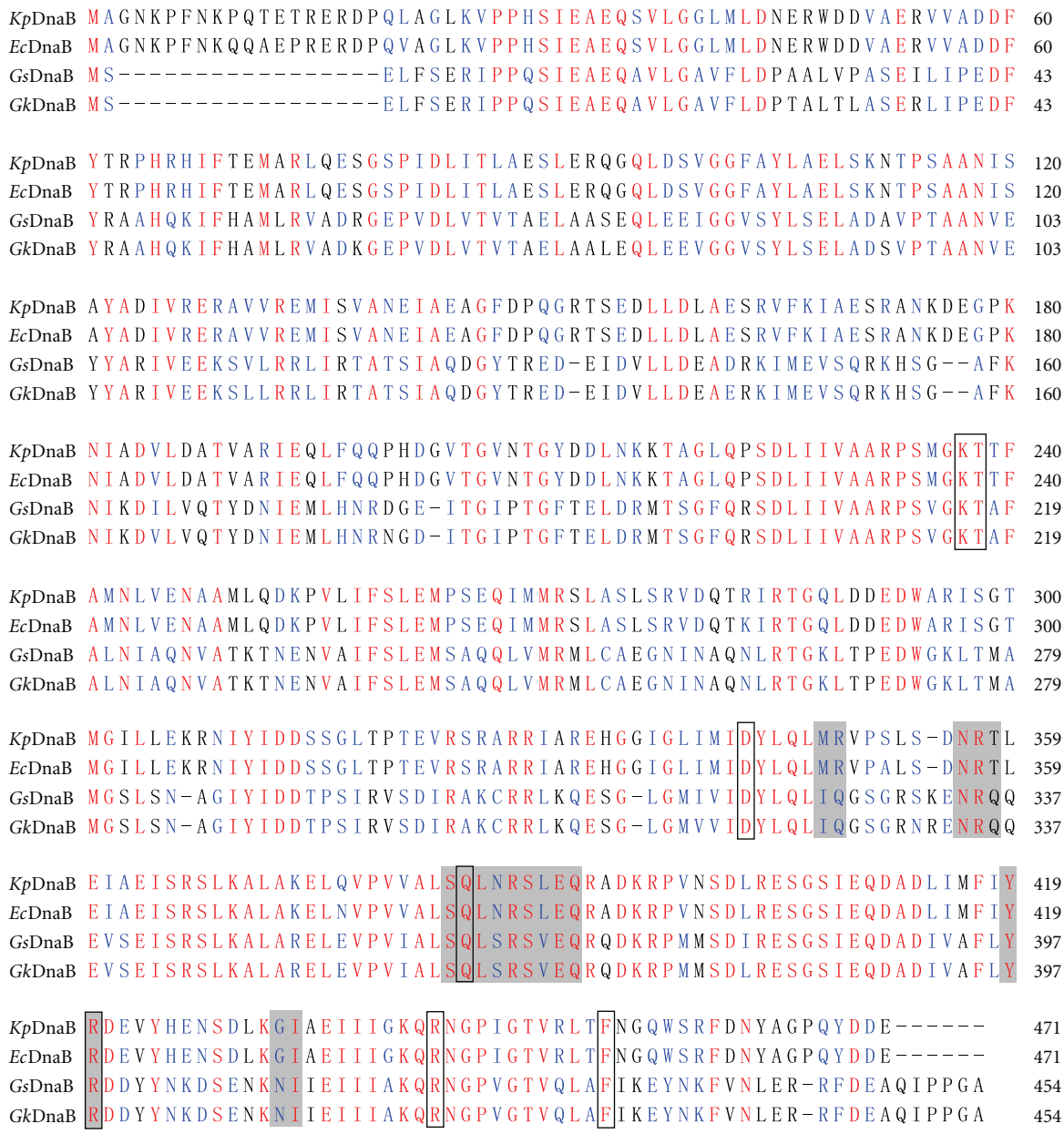

Figure 3: Multiple amino acids sequence alignment of DnaB helicases. Alignment was carried out using CLUSTALW2. Amino acid residues displaying 100% homology are highlighted in red, and those displaying similarity are highlighted in blue. The amino acids that are involved in ATP binding are boxed. The amino acids that are involved in ssDNA binding are shaded in gray. For clarity, only 4 bacterial stains are shown. Abbreviations: *Kp*, *K. pneumoniae*; *Ec*, *E. coli*; *Gs*, *Geobacillus stearothermophilus* [32]; *Gk*, *Geobacillus kaustophilus* [7].

3.4. Inhibitory Effects of Flavonols on ssDNA Binding of KpDnaB. To investigate whether the ssDNA-binding ability of *Kp*DnaB is inhibited by the flavonol, we used EMSA to study the binding of *Kp*DnaB to dT30 (Figure 5) when mixed with Myr, Que, Kae, or Gal. In the absence of any flavonol, *Kp*DnaB formed a stable complex with dT30, as shown by electrophoresis (Figure 5(a)). In the presence of 16.7 μM Gal (Figure 5(b)), Kae (Figure 5(c)), Que (Figure 5(d)), or Myr (Figure 5(e)), *Kp*DnaB still bound to dT30, but the binding activity was slightly decreased. The apparent dissociation constant ($K_{d,app}$) values of *Kp*DnaB bound to dT30 in the absence of any flavonol or presence of Myr, Que, Kae, or Gal, as determined from the titration curves, were 0.97 ± 0.07, 1.11 ± 0.05, 1.03 ± 0.07, 1.10 ± 0.05, and 1.03 ± 0.06 μM, respectively. It should be noted that the observed inhibition was dependent on protein concentration (Figure 5(f)); the disruption of formation of the *Kp*DnaB-dT30 complex did disappear when its concentration was increased to 2.72 μM, a value that the [flavonol]/[*Kp*DnaB monomer] ratio is ~6.1 (16.7/2.73 = 6.14).

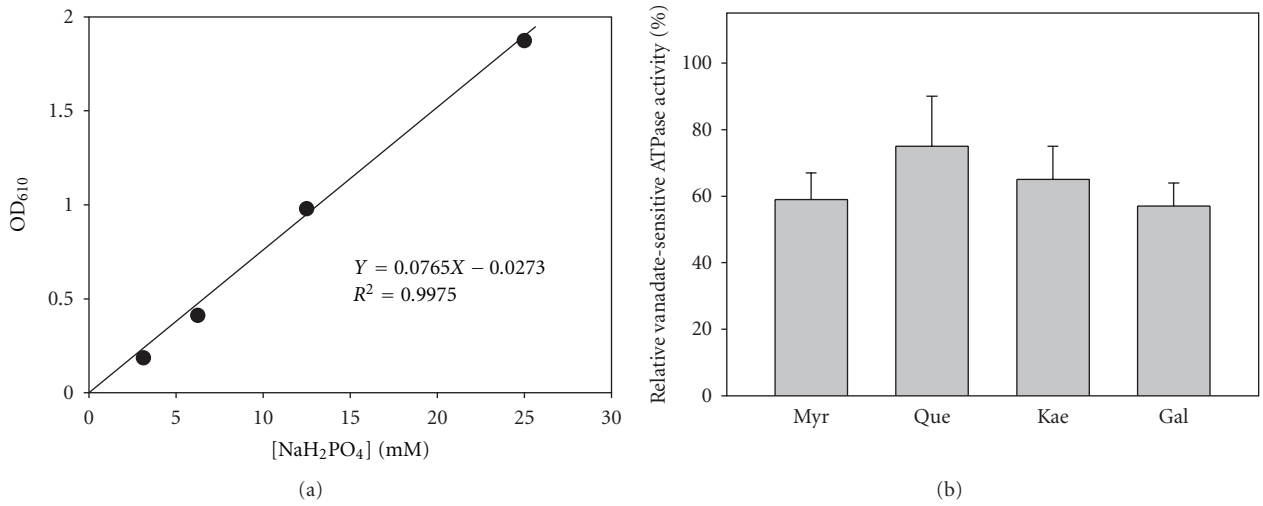

Figure 4: ssDNA-dependent ATPase activity of *Kp*DnaB. (a) The vanadate-sensitive colorimetric determination of inorganic phosphate released by the hydrolysis of ATP. A standard linear regression curve was generated by plotting the optical density (OD) at 610 nm against the concentrations of sodium phosphate (NaH_2PO_4). (b) ATPase activity of *Kp*DnaB is inhibited by flavonols. In the presence of Myr, Que, Kae, or Gal, the specific activity of *Kp*DnaB was decreased to 59%, 75%, 65%, and 57%, respectively.

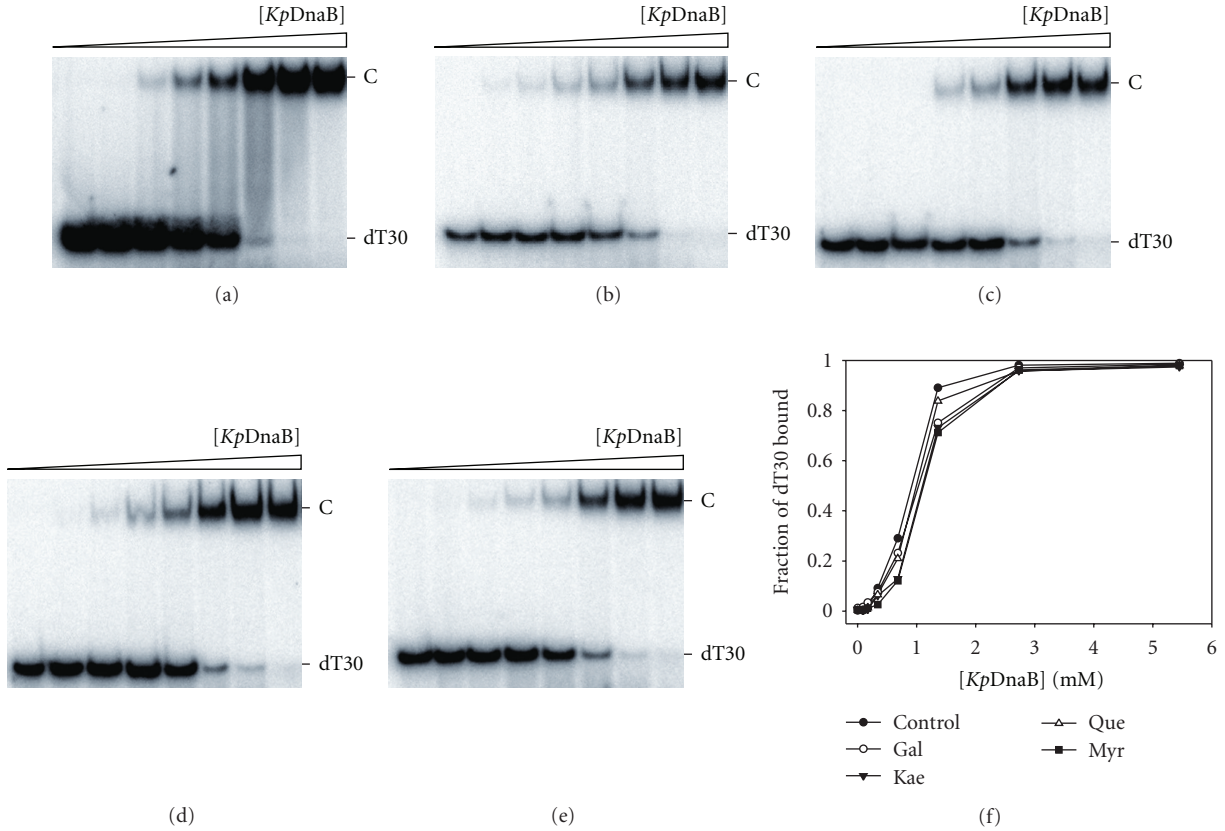

Figure 5: Inhibitory effects of flavonols on ssDNA binding of *Kp*DnaB. EMSA of *Kp*DnaB bound to dT30 (a) in the absence of any flavonol or presence of (b) Gal, (c) Kae, (d) Que, or (e) Myr. (f) The titration curves for ssDNA binding of *Kp*DnaB. The apparent dissociation constant ($K_{d,app}$) values of *Kp*DnaB bound to dT30 in the absence of any flavonol or presence of Myr, Que, Kae, or Gal, as determined from the titration curves, were 0.97 ± 0.07, 1.11 ± 0.05, 1.03 ± 0.07, 1.10 ± 0.05, and 1.03 ± 0.06 μM, respectively.

Table 1: Docking results of *Kp*DnaB with Myr and Que from PatchDock.

Solution number	Score	
	Myr	Que
1	4142	4170
2	3938	4096
3	3802	3994
4	3796	3962
5	3752	3766
6	3722	3694

3.5. Real-Time Monitoring of KpDnaB Helicase Activity Based on FRET. To investigate whether the helicase activity of *Kp*DnaB is also inhibited by flavonols, the fluorescence helicase assay was carried out in the absence or presence of Myr or Gal. This assay, modified from that for HCV NS3 3′-5′ RNA helicase [34], was found to be useful for *Kp*DnaB. The dsDNA substrate was prepared by annealing 2 oligonucleotides, a 5′ fluorophore-labeled (Alexa Fluor 488) 22-nucleotide donor and a 3′ quencher-labeled (BHQ1) 36-nucleotide quencher (Figure 6(a)). When the dsDNA substrate is unwound by the helicase, the fluorophore (F) emits upon its release from the quencher (Q). The fluorescence quenching efficiency (signal-to-background ratio) for this substrate was >90%, suggesting high sensitivity for monitoring helicase activity, similar to that for HCV NS3 RNA helicase [34].

Because of its high inhibitory effects on the ATPase activity of *Kp*DnaB (Figure 4(b)), Myr and Gal were selected for this assay. When *Kp*DnaB was added, fluorescence was continuously emitted, whereas no increase in fluorescence occurred in the absence of *Kp*DnaB (as the negative control). These results indicate that the observed fluorescence emission arose from the unwinding of the dsDNA substrate by purified *Kp*DnaB (Figure 6(b)). When assaying the helicase activity of *Kp*DnaB in the presence of Myr or Gal, a linear increase in fluorescence emission was also observed. In addition, the initial velocity for *Kp*DnaB helicase activity was nearly identical with or without flavonol ($\sim 1 \times 10^{-3}$ fluorescence intensity/s). In contrast, unlike fluorescence emission of *Kp*DnaB that continued to increase, the fluorescence emission of *Kp*DnaB assayed in the presence of the flavonol Myr or Gal soon reached its maximal point. The magnitude of fluorescence activity for *Kp*DnaB was in the following order: no flavonol added > Myr present > Gal present.

3.6. Homology Modeling. The most thoroughly studied replicative DnaB helicase from bacteria is that of *E. coli*. Although *Kp*DnaB shows a high degree of sequence identity with *Ec*DnaB, its crystal structure is not yet reported. To deeply understand the structure-function relationship of the flavonol-*Kp*DnaB-ssDNA complex(es), we decided to model its three-dimensional structure by homology modeling. The model of *Kp*DnaB was built from the coordinates of 2R6D (crystal structure of *Gs*DnaB), 2VYF (crystal structure of *Gk*DnaB) and 2VYE (crystal structure of *Gk*DnaB in complex with ssDNA) by using SWISS-MODEL, http://swissmodel.expasy.org/ [28]. *Kp*DnaB and *Gk*DnaB share 47% identity and 69%, similarity, and *Kp*DnaB and *Gs*DnaB share 46% identity and 69% similarity, respectively, in the amino acid sequences level. The three-dimensional model of the hexameric *Kp*DnaBs all forms a ring structure (Figure 7(a)), of which the loop I position in *Gk*DnaB-ssDNA complex based model was different. We propose that, as in the *Gk*DnaB complexes [7], loop I of *Kp*DnaB undergoes a conformational change, and thereby playing an important role in stabilizing DNA binding. It should be noted that the NTP-binding site, Walker A and B motifs, is adjacent to the DNA interaction site loop I (Figure 7(b)).

3.7. Docking Study Using PatchDock. The flavonol, found in DrugBank, was individually computationally docked into the three-dimensional models of *Kp*DnaB by using PatchDock, http://bioinfo3d.cs.tau.ac.il/PatchDock/ [30]. After uploading the coordinate and topology file of the flavonol and *Kp*DnaB, the docking was automatically performed. The docking results for *Kp*DnaB (*Gk*DnaB based model) interacting with Myr or Que are shown in Figure 8 and Table 1. Myr (Figure 8(a)) and Que (Figure 8(b)) were found to be docked in the ATP-binding pocket of *Kp*DnaB; however, there were also a few binding poses docked outside the pocket (Figure 8(b)). Despite a similar structure, these flavonols were found to be docked with distinct binding poses in the ATP-binding pocket of both DNA-unbound and DNA-bound models of *Kp*DnaB. For example, the binding pose of *Kp*DnaB to Myr is different from that of Que (Figure 9(a)). Que, the compound with 2 hydroxyl groups on the B ring, interacts with L214 and N215, whereas Myr (3 hydroxyl groups) interacts with L214, N247, and F460. In addition, the same compound is also found to be docked in different positions of the ATP-binding pocket of both DNA-unbound and DNA-bound models of *Kp*DnaB. For instance, Myr interacts with L214, N247, and F460 in the DNA-unbound model, and interacts with L214 and N462 in the DNA-bound model of *Kp*DnaB, respectively (Figure 9(b)). Generally, L214 is a key residue in all DNA-unbound and DNA-bound modeled structures regardless of which flavonol was used.

4. Discussion

The development of clinically useful small molecule antibiotics has been a seminal event in the world of infectious diseases [35]. DNA replication is one of the most basic biological functions and should be a prime target in antibiotic development. For example, some novel inhibitors were discovered to target topoisomerase [36, 37], DNA gyrase [38], RNA polymerase [39], helicase-primase [40], and retroviral reverse transcriptase [41, 42]. Since DNA helicases are important components of the cellular replication machinery in all organisms, inhibition of helicase activity would be detrimental to bacterial survival as well. Previously, we have shown that some flavonoid compounds can directly bind to *Kp*DnaB and inhibit its binding ability

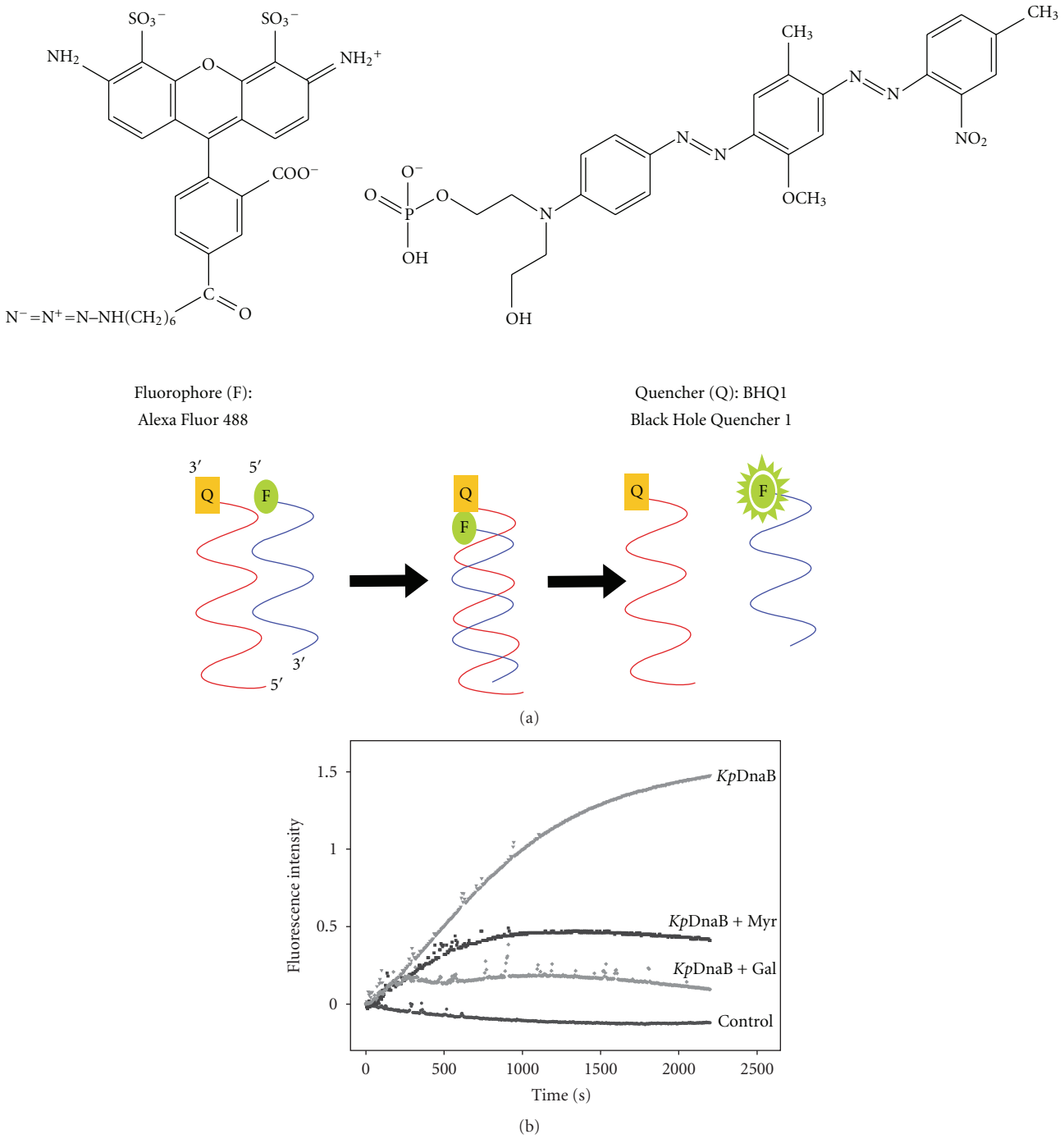

Figure 6: Real-time monitoring of *Kp*DnaB helicase activity. (a) Schematic representation of fluorescence helicase assay based on FRET. The dsDNA substrate was prepared by annealing 2 oligonucleotides, a 5′ fluorophore-labeled (Alexa Fluor 488) 22-nucleotide donor, and a 3′ quencher-labeled (BHQ1) 36-nucleotide quencher. When the dsDNA substrate is unwound by the helicase, the fluorophore (F) emits upon its release from the quencher (Q). (b) Inhibitory effects of flavonols on *Kp*DnaB helicase activity. Myr and Gal were selected for this assay.

to nucleotides, thus interfering with the growth of *K. pneumoniae* [13]. Flavonoids [14] are the most common group of plant polyphenols with antioxidant [16], antiradical [17], and antibacterial activities [18]. It is now clear that some flavonoids are ATP-inhibiting agents as competitors for ATP-binding proteins. For example, several flavonoid derivatives have been developed as therapeutic agents for cancer [43]. In this study, we used several assays to analyze the effects of 4 flavonols, namely, Myr, Que, Kae, and Gal—which contain different numbers of hydroxyl substituents on the aromatic rings—on the ssDNA binding, ATP hydrolysis, and dsDNA unwinding abilities of *Kp*DnaB. For the first

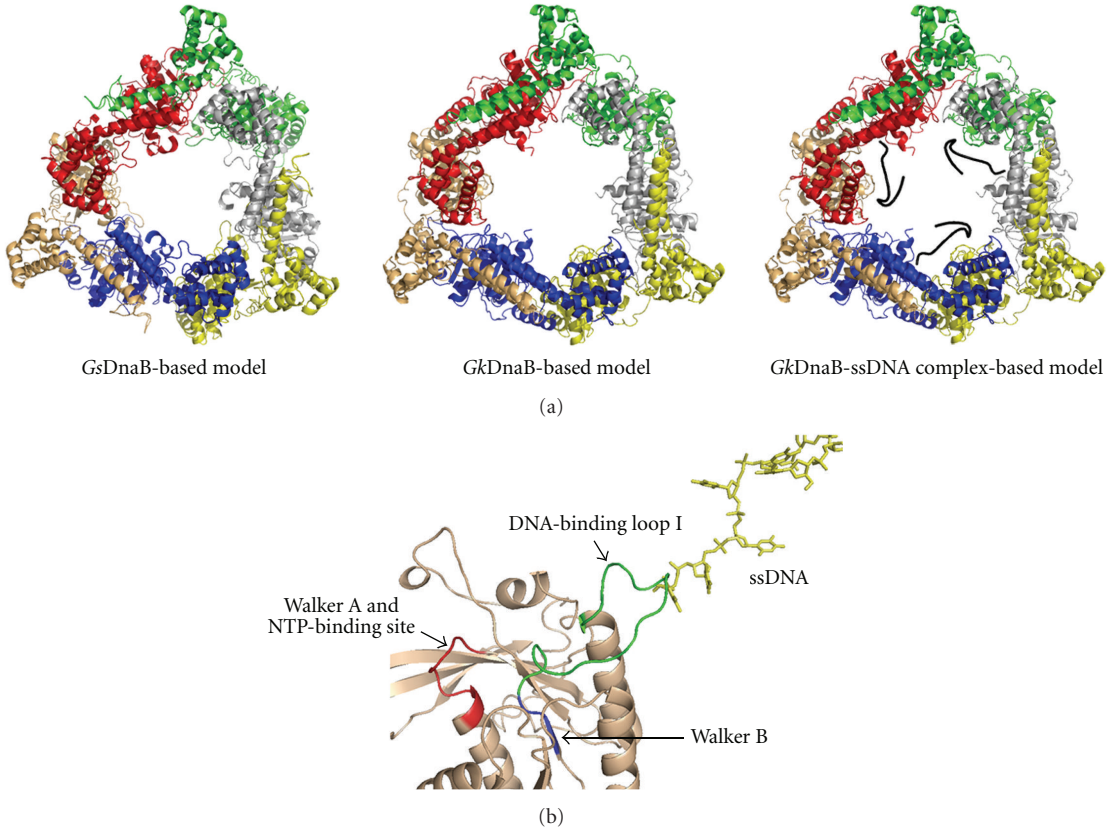

Figure 7: Homology modeling. (a) The three-dimensional models of the hexameric *Kp*DnaB form a ring structure. The monomers are colored differently. ssDNA is colored in black. (b) The structural model of the *Kp*DnaB-ssDNA complex. The NTP-binding site, Walker A and B motifs, is adjacent to the DNA interaction site loop I (green). There are synergistic effects between the nucleotide and ssDNA binding [7]. The Walker A and B motifs are colored in red and blue, respectively. ssDNA is colored in gold.

time, our results demonstrated that these flavonols were capable of inhibiting the unwinding activity of the helicase.

DnaB helicase is an ssDNA-dependent ATPase. Previously, we showed that the binding of *Kp*DnaB to dNTP is inhibited by the flavonols Myr, Kae, Gal, and Que. This study further investigated the flavonol-mediated inhibition of *Kp*DnaB binding to dNTP, which may have led to the associated decrease in ATPase activity in the presence of ssDNA (Figure 4). The ATP-hydrolyzing activity of *Kp*DnaB was inhibited by flavonols in the following order of decreasing efficiency: Gal > Myr > Kae > Que. Although it is well established that flavonoids have several hydroxyl groups, and thus have marked potentials to bind any protein, the strength of inhibition of *Kp*DnaB ATP-hydrolyzing activity did not correlate with the number of hydroxyl substituents on the flavonol aromatic rings. In addition, the structural model of *Kp*DnaB shows that these flavonols bind to *Kp*DnaB with distinct binding poses in the ATP-binding pocket (Figure 9). This situation is also found in several ATP-binding proteins that bind to different flavonoids. Crystal structures of PIM1 kinase in complex with quercetagetin and Myr reveal 2 distinct binding poses in the ATP-binding pocket, namely, orientations I and II [44]. Myr, adopting orientation II, has flipped 180° in PIM1 kinase, in contrast to quercetagetin (orientation I), such that the B ring is oriented toward the entrance of the ATP pocket. These orientations in PIM1 are also found to closely resemble those of Que and Myr in phosphatidylinositol 3-kinase [45]. Although the ATP-binding pocket in these proteins, including *Kp*DnaB, is different, cases of PIM1 and phosphatidylinositol 3-kinase with different binding poses, are very similar to that of *Kp*DnaB. Despite a very similar structure, flavonols may bind to *Kp*DnaB by using different mechanisms, as shown in the structural models (Figures 8 and 9). This may explain why the strength of inhibition in *Kp*DnaB ATPase activity was not correlated with the number of hydroxyl substituents on the flavonol aromatic rings.

Other studies showed that Myr noncompetitively inhibits *E. coli* DnaB helicase with an IC_{50} of approximately 10 μM [46]; however, we have recently discovered that Gal, Kae, Que, and Myr can inhibit dNTP binding to *Kp*DnaB, indicating a specific inhibitory process. Furthermore, these flavonols can be docked into the *Kp*DnaB ATP-binding pocket. It is not known whether this disparity is due to the inherent differences among the species, or an alternative (allosteric) binding site(s) in DnaB helicase. However, the docking results also show that a few binding poses of the flavonol outside the ATP-binding pocket

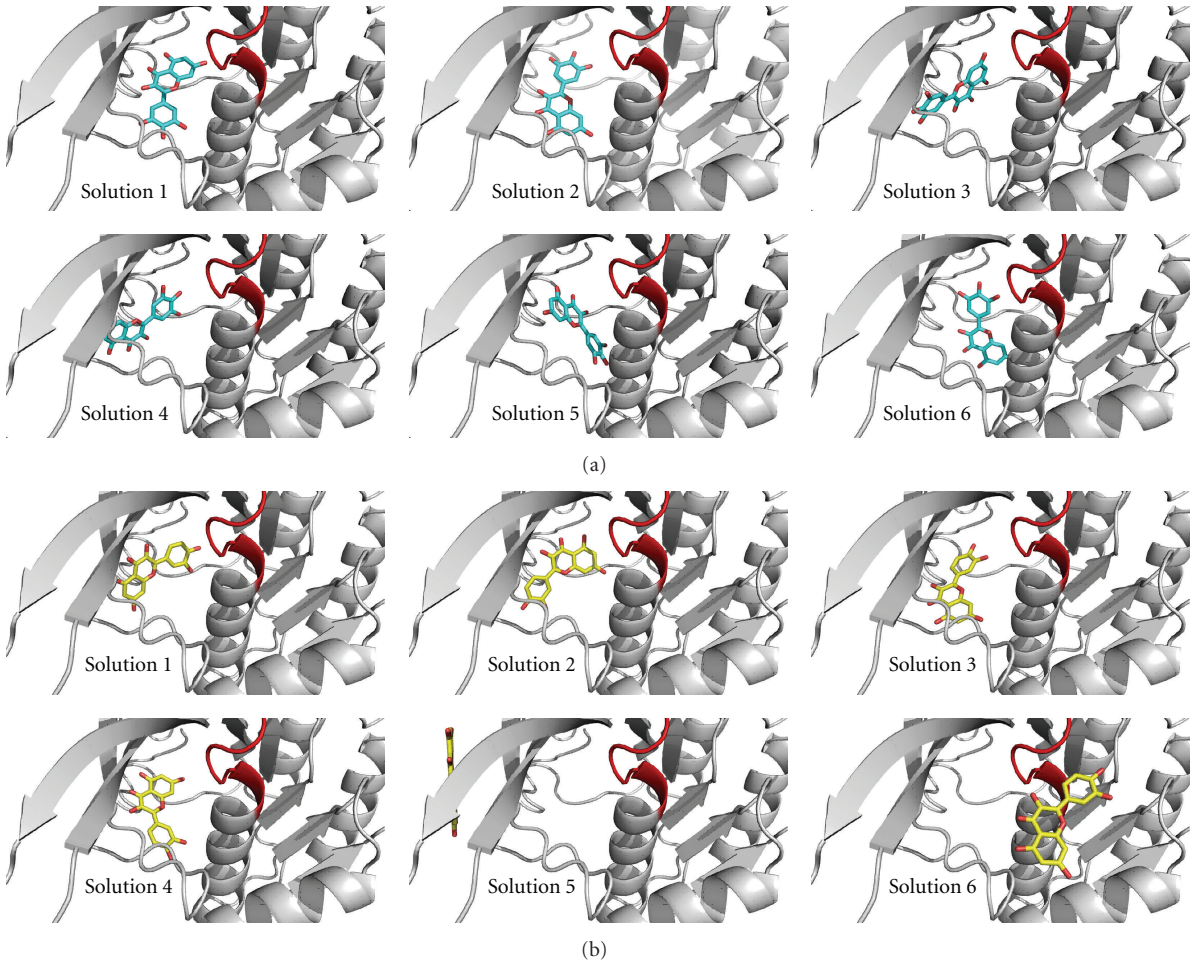

FIGURE 8: Representation of the docking models from PatchDock. The six docking models with the highest score for *Kp*DnaB (*Gk*DnaB-based model) interacting with (a) Myr and (b) Que are shown. The Walker A motif (aa 232–238), a nucleotide binding site, is colored in red.

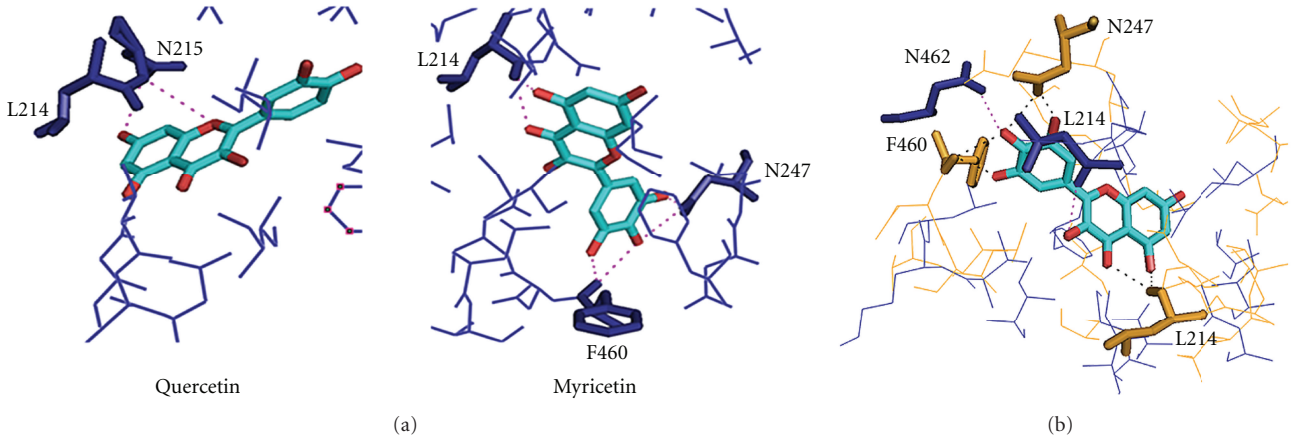

FIGURE 9: (a) The binding pose of *Kp*DnaB to Myr is different from that of Que. Que interacts with L214 and N215, whereas Myr interacts with L214, N247, and F460. (b) Myr was docked in different positions of the ATP-binding pocket of both DNA-unbound and DNA-bound models of *Kp*DnaB. Myr interacts with L214, N247, and F460 in the DNA-unbound model, and interacts with L214 and N462 in the DNA-bound model of *Kp*DnaB, respectively.

(Figure 8), suggesting that there may be more than one site for flavonol binding in the DnaB helicase. This may explain why Myr non-competitively inhibits *Ec*DnaB. In addition, we also showed flavonol-mediated inhibition of *Kp*DnaB-ssDNA complex formation, which depended on the [flavonol]/[*Kp*DnaB monomer] ratio; at a ~6 fold ratio, the inhibitory effect did disappear (Figure 5). Since these flavonols inhibited not only the ATPase activity of *Kp*DnaB but also the ssDNA-binding ability, we believe that there may be more than one site in *Kp*DnaB for flavonol binding. However, this speculation must be confirmed by further biochemical experiments.

In this study, we describe a new in vitro fluorescence assay for measuring 5′-3′ DNA helicase activity by using dsDNA substrate (Figure 6). Alexa Fluor 488 and BHQ1 were selected as the fluorophore-quencher pair. This assay enables the real-time, high-throughput measurement of DNA helicase activity, and does not require time-consuming procedures like the conventional gel-based assays. For example, on the basis of this assay, we observed that the initial velocity of *Kp*DnaB for the unwinding activity assayed in the absence of the flavonol, or with Myr or Gal were very similar; however, their maximal activities were different. While fluorescence was continuously emitted without the addition of flavonol to the *Kp*DnaB solution, the fluorescence increase stopped at ~300 s and ~600 s for Myr and Gal, respectively (Figure 6(b)). This real-time unwinding kinetics of the DNA helicase cannot be easily observed by the conventional gel-based assays. Our laboratory is currently screening DNA helicase inhibitors using this high-throughput method.

All DNA-unbound and DNA-bound modeled structures showed flavonols binding to *Kp*DnaB with distinct poses. However, these models all displayed a key residue involved in the flavonol binding, namely, L214. The L214 residue in DnaB helicases is highly conserved (Figure 3), but its role has not yet been determined. On the basis of these results, we propose that these flavonols may inhibit *Kp*DnaB in 2 possible ways. First, since DnaB helicase binding to dNTP causes a large conformational change [31, 47, 48] to become a translocase [7], these flavonols may partially occupy the ATP-binding pocket of the DnaB helicase and inhibit conformational change, thereby causing varying degrees of inhibition. This is a possible inhibition mechanism because the L214 residue of *Kp*DnaB is not involved in ATP binding (Figure 3), but most structural models indicate its importance in binding flavonols (Figure 9). Second, more than one flavonol binds to *Kp*DnaB; 1 is at the active site, and the other(s) is at an unknown site. The overall inhibition possibly results from the interactions between the flavonols and the enzyme. This may be a reason why flavonols not only bind at the ATP pocket of the DNA helicase, but can also non-competitively inhibit the ATPase activity of the DNA helicase [46]. Our crystal structure of *Gk*DnaB in complex with ssDNA previously suggested that ATP hydrolysis may drive the movement of the helicase toward the 3′ end of the lagging strand [7]. In addition, the dNTP-binding site of the helicase at loop I, part of the Walker B motif, is adjacent to the DNA interaction site. In conclusion, the flavonol likely inhibits the DNA helicase (translocase) activity by affecting the ATP binding of *Kp*DnaB, to ultimately shut down and lock the enzyme in the ATP-unbound state.

Acknowledgments

The authors thank Ms. Yen-Hua Huang for structural modeling and docking. This research was supported by a grant from the National Research Program for Genome Medicine, Taiwan (NSC 100-3112-B-040-001 to C.-Y. Huang).

References

[1] R. Reyes-Lamothe, D. J. Sherratt, and M. C. Leake, "Stoichiometry and architecture of active DNA replication machinery in *Escherichia coli*," *Science*, vol. 328, no. 5977, pp. 498–501, 2010.

[2] M. L. Mott and J. M. Berger, "DNA replication initiation: mechanisms and regulation in bacteria," *Nature Reviews Microbiology*, vol. 5, no. 5, pp. 343–354, 2007.

[3] K. J. Marians, "Prokaryotic DNA replication," *Annual Review of Biochemistry*, vol. 61, pp. 673–719, 1992.

[4] T. A. Baker and S. P. Bell, "Polymerases and the replisome: machines within machines," *Cell*, vol. 92, no. 3, pp. 295–305, 1998.

[5] M. R. Singleton, M. S. Dillingham, and D. B. Wigley, "Structure and mechanism of helicases and nucleic acid translocases," *Annual Review of Biochemistry*, vol. 76, pp. 23–50, 2007.

[6] S. S. Patel and K. M. Picha, "Structure and function of hexameric helicases," *Annual Review of Biochemistry*, vol. 69, pp. 651–697, 2000.

[7] Y. H. Lo, K. L. Tsai, Y. J. Sun, W. T. Chen, C. Y. Huang, and C. D. Hsiao, "The crystal structure of a replicative hexameric helicase DnaC and its complex with single-stranded DNA," *Nucleic Acids Research*, vol. 37, no. 3, pp. 804–814, 2009.

[8] H. W. Boucher, G. H. Talbot, J. S. Bradley et al., "Bad bugs, no drugs: no ESKAPE! An update from the Infectious Diseases Society of America," *Clinical Infectious Diseases*, vol. 48, no. 1, pp. 1–12, 2009.

[9] K. K. Kumarasamy, M. A. Toleman, T. R. Walsh et al., "Emergence of a new antibiotic resistance mechanism in India, Pakistan, and the UK: a molecular, biological, and epidemiological study," *The Lancet Infectious Diseases*, vol. 10, no. 9, pp. 597–602, 2010.

[10] K. Bush, "Alarming β-lactamase-mediated resistance in multidrug-resistant *Enterobacteriaceae*," *Current Opinion in Microbiology*, vol. 13, no. 5, pp. 558–564, 2010.

[11] R. Podschun and U. Ullmann, "*Klebsiella* spp. as nosocomial pathogens: epidemiology, taxonomy, typing methods, and pathogenicity factors," *Clinical Microbiology Reviews*, vol. 11, no. 4, pp. 589–603, 1998.

[12] P. Soultanas, "The bacterial helicase-primase interaction: a common structural/functional module," *Structure*, vol. 13, no. 6, pp. 839–844, 2005.

[13] C. C. Chen and C. Y. Huang, "Inhibition of *Klebsiella pneumoniae* dnab helicase by the flavonol galangin," *Protein Journal*, vol. 30, no. 1, pp. 59–65, 2011.

[14] J. A. Ross and C. M. Kasum, "Dietary flavonoids: bioavailability, metabolic effects, and safety," *Annual Review of Nutrition*, vol. 22, pp. 19–34, 2002.

[15] F. Teillet, A. Boumendjel, J. Boutonnat, and X. Ronot, "Flavonoids as RTK inhibitors and potential anticancer agents," *Medicinal Research Reviews*, vol. 28, no. 5, pp. 715–745, 2008.

[16] K. L. Wolfe and R. H. Liu, "Structure-activity relationships of flavonoids in the cellular antioxidant activity assay," *Journal of Agricultural and Food Chemistry*, vol. 56, no. 18, pp. 8404–8411, 2008.

[17] S. Burda and W. Oleszek, "Antioxidant and antiradical activities of flavonoids," *Journal of Agricultural and Food Chemistry*, vol. 49, no. 6, pp. 2774–2779, 2001.

[18] T. P. T. Cushnie and A. J. Lamb, "Antimicrobial activity of flavonoids," *International Journal of Antimicrobial Agents*, vol. 26, no. 5, pp. 343–356, 2005.

[19] C. C. Wang, H. W. Tsau, W. T. Chen, and C. Y. Huang, "Identification and characterization of a putative dihydroorotase, KPN01074, from *Klebsiella pneumoniae*," *Protein Journal*, vol. 29, no. 6, pp. 445–452, 2010.

[20] H. C. Jan, Y. L. Lee, and C. Y. Huang, "Characterization of a single-stranded DNA-binding protein from *Pseudomonas aeruginosa* PAO1," *Protein Journal*, vol. 30, no. 1, pp. 20–26, 2011.

[21] Y. H. Huang, Y. L. Lee, and C. Y. Huang, "Characterization of a single-stranded DNA binding protein from *Salmonella* enterica serovar typhimurium LT2," *Protein Journal*, vol. 30, no. 2, pp. 102–108, 2011.

[22] Y. H. Huang and C. Y. Huang, "Characterization of a single-stranded DNA binding protein from *Klebsiella pneumoniae*: mutation at either Arg73 or Ser76 causes a less cooperative complex on DNA," *Genes to Cells*, vol. 17, pp. 146–157, 2012.

[23] H. C. Hsieh and C. Y. Huang, "Identification of a novel protein, PriB, in *Klebsiella pneumoniae*," *Biochemical and Biophysical Research Communications*, vol. 404, no. 1, pp. 546–551, 2011.

[24] C. Y. Huang, C. H. Hsu, Y. J. Sun, H. N. Wu, and C. D. Hsiao, "Complexed crystal structure of replication restart primosome protein PriB reveals a novel single-stranded DNA-binding mode," *Nucleic Acids Research*, vol. 34, no. 14, pp. 3878–3886, 2006.

[25] J. H. Liu, T. W. Chang, C. Y. Huang et al., "Crystal structure of PriB, a primosomal DNA replication protein of *Escherichia coli*," *Journal of Biological Chemistry*, vol. 279, no. 48, pp. 50465–50471, 2004.

[26] P. P. Van Veldhoven and G. P. Mannaerts, "Inorganic and organic phosphate measurements in the nanomolar range," *Analytical Biochemistry*, vol. 161, no. 1, pp. 45–48, 1987.

[27] M. A. Larkin, G. Blackshields, N. P. Brown et al., "Clustal W and Clustal X version 2.0," *Bioinformatics*, vol. 23, no. 21, pp. 2947–2948, 2007.

[28] K. Arnold, L. Bordoli, J. Kopp, and T. Schwede, "The SWISS-MODEL workspace: a web-based environment for protein structure homology modelling," *Bioinformatics*, vol. 22, no. 2, pp. 195–201, 2006.

[29] C. Knox, V. Law, T. Jewison et al., "DrugBank 3.0: a comprehensive resource for 'Omics' research on drugs," *Nucleic Acids Research*, vol. 39, no. 1, pp. D1035–D1041, 2011.

[30] D. Schneidman-Duhovny, Y. Inbar, R. Nussinov, and H. J. Wolfson, "PatchDock and SymmDock: servers for rigid and symmetric docking," *Nucleic Acids Research*, vol. 33, no. 2, pp. W363–W367, 2005.

[31] A. Roychowdhury, M. R. Szymanski, M. J. Jezewska, and W. Bujalowski, "Mechanism of NTP hydrolysis by the *Escherichia coli* primary replicative helicase DnaB protein. 2. Nucleotide and nucleic acid specificities," *Biochemistry*, vol. 48, no. 29, pp. 6730–6746, 2009.

[32] S. Bailey, W. K. Eliason, and T. A. Steitz, "Structure of hexameric DnaB helicase and its complex with a domain of DnaG primase," *Science*, vol. 318, no. 5849, pp. 459–463, 2007.

[33] E. E. Biswas and S. B. Biswas, "Mechanism of DnaB helicase of *Escherichia coli*: structural domains involved in ATP hydrolysis, DNA binding, and oligomerization," *Biochemistry*, vol. 38, no. 34, pp. 10919–10928, 1999.

[34] H. Tani, O. Fujita, A. Furuta et al., "Real-time monitoring of RNA helicase activity using fluorescence resonance energy transfer in vitro," *Biochemical and Biophysical Research Communications*, vol. 393, no. 1, pp. 131–136, 2010.

[35] A. Koul, E. Arnoult, N. Lounis, J. Guillemont, and K. Andries, "The challenge of new drug discovery for tuberculosis," *Nature*, vol. 469, no. 7331, pp. 483–490, 2011.

[36] B. D. Bax, P. F. Chan, D. S. Eggleston et al., "Type IIA topoisomerase inhibition by a new class of antibacterial agents," *Nature*, vol. 466, no. 7309, pp. 935–940, 2010.

[37] M. T. Black and K. Coleman, "New inhibitors of bacterial topoisomerase GyrA/ParC subunits," *Current Opinion in Investigational Drugs*, vol. 10, no. 8, pp. 804–810, 2009.

[38] K. L. Hopkins, R. H. Davies, and E. J. Threlfall, "Mechanisms of quinolone resistance in *Escherichia coli* and *Salmonella*: recent developments," *International Journal of Antimicrobial Agents*, vol. 25, no. 5, pp. 358–373, 2005.

[39] A. Srivastava, M. Talaue, S. Liu et al., "New target for inhibition of bacterial RNA polymerase: 'switch region'," *Current Opinion in Microbiology*, vol. 14, no. 5, pp. 532–543, 2011.

[40] K. Chono, K. Katsumata, T. Kontani et al., "ASP2151, a novel helicase-primase inhibitor, possesses antiviral activity against varicella-zoster virus and herpes simplex virus types 1 and 2," *Journal of Antimicrobial Chemotherapy*, vol. 65, no. 8, Article ID dkq198, pp. 1733–1741, 2010.

[41] S. Li, T. Hattori, and E. N. Kodama, "Epigallocatechin gallate inhibits the HIV reverse transcription step," *Antiviral Chemistry and Chemotherapy*, vol. 21, no. 6, pp. 239–243, 2011.

[42] S. C. Chu, Y. S. Hsieh, and J. Y. Lin, "Inhibitory effects of flavonoids on moloney murine leukemia virus reverse transcriptase activity," *Journal of Natural Products*, vol. 55, no. 2, pp. 179–183, 1992.

[43] M. K. Chahar, N. Sharma, M. P. Dobhal, and Y. C. Joshi, "Flavonoids: a versatile source of anticancer drugs," *Pharmacognosy Reviews*, vol. 5, no. 9, pp. 1–12, 2011.

[44] S. Holder, M. Zemskova, C. Zhang et al., "Characterization of a potent and selective small-molecule inhibitor of the PIM1 kinase," *Molecular Cancer Therapeutics*, vol. 6, no. 1, pp. 163–172, 2007.

[45] E. H. Walker, M. E. Pacold, O. Perisic et al., "Structural determinants of phosphoinositide 3-kinase inhibition by wortmannin, LY294002, quercetin, myricetin, and staurosporine," *Molecular Cell*, vol. 6, no. 4, pp. 909–919, 2000.

[46] M. A. Griep, S. Blood, M. A. Larson, S. A. Koepsell, and S. H. Hinrichs, "Myricetin inhibits *Escherichia coli* DnaB helicase but not primase," *Bioorganic and Medicinal Chemistry*, vol. 15, no. 22, pp. 7203–7208, 2007.

[47] M. J. Jezewska, U. S. Kim, and W. Bujalowski, "Interactions of *Escherichia coli* primary replicative helicase DnaB protein with nucleotide cofactors," *Biophysical Journal*, vol. 71, no. 4, pp. 2075–2086, 1996.

[48] M. J. Jezewska and W. Bujalowski, "Global conformational transitions in *Escherichia coli* primary replicative helicase DnaB protein induced by ATP, ADP, and single-stranded DNA binding: multiple conformational states of the helicase hexamer," *Journal of Biological Chemistry*, vol. 271, no. 8, pp. 4261–4265, 1996.